LINKING METEOROLOGY, TURBULENCE, AND AIR CHEMISTRY IN THE AMAZON RAIN FOREST

BY JOSE D. FUENTES, MARCELO CHAMECKI, ROSA MARIA NASCIMENTO DOS SANTOS, CELSO VON RANDOW, PAUL C. STOY, GABRIEL KATUL, DAVID FITZJARRALD, ANTONIO MANZI, TOBIAS GERKEN, AMY TROWBRIDGE, LIVIA SOUZA FREIRE, JESUS RUIZ-PLANCARTE, JAIR MAX FURTUNATO MAIA, JULIO TÓTA, NELSON DIAS, GILBERTO FISCH, COURTNEY SCHUMACHER, OTAVIO ACEVEDO, JULIANE REZENDE MERCER, AND ANA MARIA YAÑEZ-SERRANO

A field campaign reveals that the Amazon rain forest produces enough chemical species to undergo oxidation and generate aerosols, which can activate into cloud condensation nuclei and potentially influence cloud formation.

The objectives of this article are to describe the principal features of a field campaign in the central Amazonia rain forest of Brazil and to highlight the key findings to date. The field project was designed i) to investigate the influences of atmospheric turbulence on the transport and distribution of rain forest–emitted hydrocarbons using an array of sensors deployed within and above the canopy (Fig. 1), ii) to determine the chemical processing of rain forest–emitted hydrocarbons due to reactions with ozone and hydroxyl within the forest, and iii) to study the gas-to-particle conversion and associated

AFFILIATIONS: FUENTES, CHAMECKI, GERKEN, SOUZA FREIRE, AND RUIZ-PLANCARTE—The Pennsylvania State University, University Park, Pennsylvania; NASCIMENTO DOS SANTOS AND FURTUNATO MAIA—Universidade do Estado do Amazonas, Manaus, Brazil; VON RANDOW—National Institute for Space Research (INPE), São José dos Campos, Brazil; STOY AND REZENDE MERCER—Montana State University, Bozeman, Montana; KATUL—Duke University, Durham, North Carolina; FITZJARRALD—Atmospheric Sciences Research Center, University at Albany, State University of New York, Albany, New York; MANZI AND YAÑEZ-SERRANO—Instituto Nacional de Pesquisas da Amazônia, Manaus, Brazil; TROWBRIDGE—Indiana University, Bloomington, Indiana; TÓTA—Universidade Federal do Oeste do Pará (UFOPA), Santarém, Brazil; DIAS—Universidade Federal do Paraná (UFPR), Curitiba, Brazil; FISCH—Instituto de Aeronaútica e Espaço, Departamento de Ciência e Tecnologia Aeroespacial, São Paulo, Brazil; SCHUMACHER—Texas A&M University, College Station, Texas; ACEVEDO—Federal University of Santa Maria (UFSM), Santa Maria, Brazil
CORRESPONDING AUTHOR: Jose D. Fuentes, Department of Meteorology and Atmospheric Science, The Pennsylvania State University, 508 Walker Bldg., University Park, PA 16802
E-mail: jdfuentes@psu.edu

The abstract for this article can be found in this issue, following the table of contents.

DOI:10.1175/BAMS-D-15-00152.1

In final form 23 May 2016

cloud condensation nuclei yield during both wet and dry seasons in the central Amazon. This article is part of the GoAmazon project, whose research objectives and field deployments of ground- and airborne-based observing systems are described in Martin et al. (2016).

The Amazon rain forest experiences mass, momentum, and energy exchanges that directly influence deep atmospheric convection. These exchanges lead to teleconnections with other regions and are an important part of the Earth's climate system (Nobre et al. 1991; Werth and Avissar 2002). By virtue of its expansive and somewhat intact forests endowed with diverse plant species, the Amazon emits many different hydrocarbon compounds in large amounts (e.g., Guenther et al. 1995; Zimmerman et al. 1988; Kesselmeier et al. 2002; Kuhn et al. 2002; Jardine et al. 2011; Jardine et al. 2015), including isoprene, monoterpenes, sesquiterpenes, and oxygenated hydrocarbons. In the presence of nitrogen oxides, the photooxidation of plant-emitted hydrocarbons can enhance the formation of oxidants, acids, and aerosols (Fuentes et al. 2000). Hydrocarbons can react with ozone, hydroxyl, and nitrate radicals, leading to the formation of oxidants and secondary organic aerosols (SOAs) that represent a substantial fraction of the aerosol loadings in the Amazon (Andreae et al. 2004; Pöschl et al. 2010). SOAs can activate and become cloud condensation nuclei (CCN) in the presence of sulfuric or nitric acid.

In the Amazon region, aerosol concentrations remain relatively low (Andreae et al. 2002; Martin et al. 2010). These low aerosol concentrations, particularly during the wet season, cause the Amazonian cloud microphysical processes to exhibit similar traits to tropical marine environments (Roberts et al. 2001) and as such it is hypothesized to behave as a "green ocean" (Williams et al. 2002). Features such as biomass burning, predominantly during the dry season, can perturb the conditions exemplified during the wet season, resulting in seasonal dynamics of green ocean characteristics that remain partially understood (Machado et al. 2014). Questions still remain as to whether sufficient CCN are formed in the absence of biomass burning to influence convective precipitation during both wet and dry seasons.

Forest–atmosphere interactions, as depicted in Fig. 1, control both the flux and the chemistry of rain forest–emitted hydrocarbons and the oxidative state of the troposphere and, thus, need to be investigated to better understand the large-scale processes impacting tropical convection and precipitation processes. At the leaf and plant levels, hydrocarbon emissions are controlled by foliage temperature, soil moisture content, incident photosynthetic active irradiance, and phenology. Turbulent motions then govern the atmospheric transport of these compounds from sites of gas emission to the canopy air space and eventually to the overlying atmospheric boundary layer (ABL). Leaf area and its vertical distribution, tree density, and sensible and latent heat fluxes exert control on the intensity of the turbulence within and immediately above the canopy (Finnigan 2000). As a result of characteristically high leaf area indices (>4 m^2 m^{-2}), mature rain forests experience low vertical velocity fluctuations as expressed by the mean standard deviation of the vertical velocity σ_w in the lower region of the canopy (e.g., Kruijt et al. 2000). However, energetically strong eddies intermittently penetrate the canopy top (Fig. 1) and promote enhanced exchanges of air masses between the forest and the overlying atmosphere (Kaimal and Finnigan 1994). Air parcel sweeps into the canopy and ejections from the canopy are common features in tall forests (Fig. 1). In-canopy levels of turbulence yield air parcel residence times on the order of minutes (Strong et al. 2004; Fuentes et al. 2007), which are comparable to the lifetimes of plant-emitted hydrocarbons. In addition, forest–atmosphere coherent exchanges of momentum and mass, as quantified by the duration of an ejection-sweep cycle, are also on the order of minutes (Dupont and Brunet 2009; Katul et al. 2006). Hence, depending on air parcel residence times, some fraction of locally emitted hydrocarbons can be chemically destroyed before gases are vented out of the canopy (Fuentes et al. 2007) and eventually into the overlying atmospheric boundary layer (Fig. 1). Because of the complex interplay of these processes and the wide distribution of residence time scales, it is necessary to resolve intermittent and localized coherent motions within and above tropical forest canopies to understand the chemistry of the atmospheric boundary layer in the Amazon. It is envisaged that coupled turbulence–atmospheric chemistry models can be improved by resolving forest–atmosphere hydrocarbon, heat, and moisture exchanges.

Once air parcels are ejected out of the canopy (Fig. 1), concentrations of reactive trace gases and aerosols in the atmospheric boundary layer are modulated by entrainment of free-atmospheric air at the top of the boundary layer and synoptic-scale advection. Mixing within the atmospheric boundary layer and across its upper interface tends to drive reactive constituents away from chemical equilibrium. Therefore, the aerosol vertical distribution within the daytime atmospheric boundary layer is determined by aerosol formation, deposition onto the forest canopy, turbulent transport characteristics within the boundary

layer, and escape from the atmospheric boundary layer capping inversion (Fig. 1). These processes frame the overarching theme of the field project described in this manuscript.

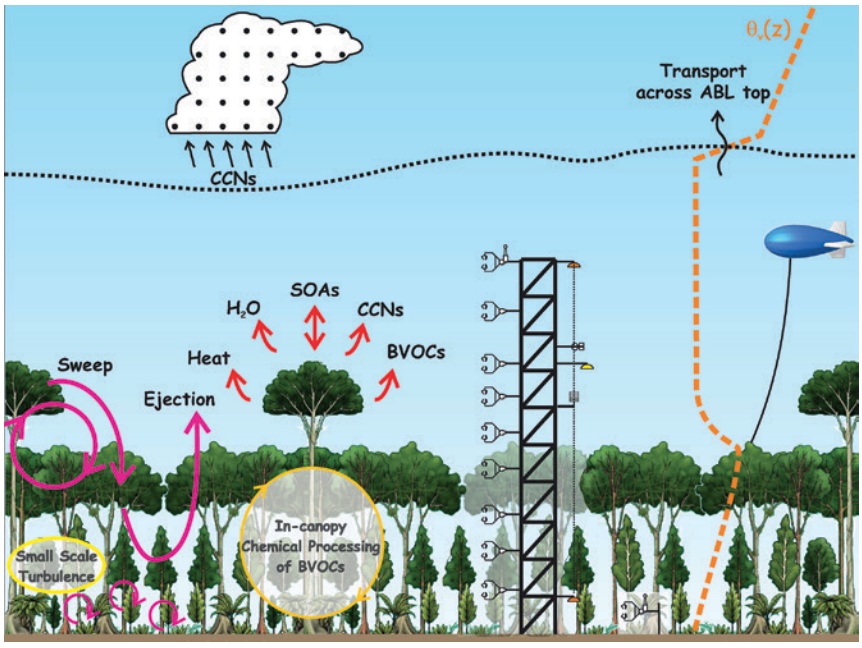

Fig. 1. An illustration of the processes associated with BVOC emissions, SOAs, and CCN formation, and the setup of instruments used to study photooxidation, chemical processing, and the transport of atmospheric constituents in a remote Amazonian rain forest. The vertical dashed line represents a characteristic daytime profile of the virtual potential temperature [θ_v(z)] and the horizontal dashed line represents the top of the ABL.

RESEARCH SITE DESCRIPTION AND INSTRUMENTATION. The field campaign took place at the Cuieiras Biological Reserve (–2.60191° latitude, –60.2093° longitude; Fig. 2). The site is located approximately 60 km north-northwest of the city of Manaus and is managed by the Brazilian National Institute for Amazon Research (INPA). A 50-m-tall tower (known as the K34 tower) served as a platform to mount instruments to investigate atmospheric turbulence and chemistry within and above the rain forest. The research site is in a dense rain forest with maximum tree heights ranging from 30 to 40 m. The leaf area index is estimated between 6.1 (Marques Filho et al. 2005) and 7.3 m^2 m^{-2} (Tóta et al. 2012), depending on measurement method and site location.

Measurements were made from April 2014 to January 2015. To investigate the air turbulence within and above the forest canopy, nine triaxial sonic anemometers (model CSAT3, Campbell Scientific, Inc., Logan, Utah) were deployed on the meteorological tower (Fig. 2) and one on a nearby 3-m subcanopy tower. Sonic anemometers provided zonal u, meridional υ, and vertical w wind speed, as well as virtual sonic temperature [T_v; it is the temperature calculated from the speed of sound provided by the sonic anemometer; Kaimal and Gaynor (1991)]. With these measurements (Table 1), turbulence statistics (e.g., σ_w) within the canopy (or roughness) sublayer can be determined (Kruijt et al. 2000). Likewise, forest–atmosphere exchanges of momentum ($\tau = \rho u_*^2$, where u_* is the friction velocity at the canopy top, and

$$u_* = \left[\left(\overline{u'w'}\right)^2 + \left(\overline{\upsilon'w'}\right)^2\right]^{1/4},$$

where primes represent deviations from the mean values) and sensible heat H were calculated. Sonic anemometers at the lower- and uppermost levels were accompanied with infrared gas analyzers (models LI-7500A and LI-7200, LI-COR Inc., Lincoln, Nebraska) to provide the information necessary to calculate the latent heat LE and carbon dioxide flux densities near the forest floor and above the canopy. The surface energy balance components, including the net radiation (R_{Net}; model CNR1, Kipp & Zonen, Delft, the Netherlands) were measured at 1.5 m above the forest floor and at 39 m above the ground. Soil heat flux plates (model HFP01SC, Hukseflux Thermal Sensors B.V., Delft, the Netherlands) were placed at different depths (Table 1) to provide energy flux densities into the soil.

Atmospheric trace gases and aerosols were sampled at 40 m above the ground. Ambient levels of ozone, nitrogen oxides [NO_x = NO (nitric oxide) + NO_2 (nitrogen dioxide)], sulfur dioxide (SO_2), and carbon monoxide (CO; models 49i, 42i-TL, 43i-TLE, and 48i; Thermo Fisher Scientific, Waltham, Massachusetts) were measured continuously at the frequency of 1 Hz. A high-sensitivity Proton Transfer Reaction Mass Spectrometer (PTR-MS; Ionicon Analytik GmbH, Innsbruck, Austria) provided hydrocarbon species and concentrations from the air intake placed 40 m above the ground. Because the

Fig. 2. (top) A panoramic view of the rain forest. (bottom left) Ten 3D sonic anemometers were deployed on a 50-m tower to study air turbulence. (bottom center left) Net radiation measurements were made 1.5 m above the forest floor and at 39 m above the ground to study the surface energy balance. (bottom center right) Sonic anemometers at the lower- and uppermost levels were accompanied with gas analyzers to provide information for calculating evapotranspiration near the forest floor and above the canopy. (bottom right) An air inlet, placed at 40 m above the ground, allowed air sampling for trace gases above the forest.

PTR-MS only characterizes compounds and fractions of compounds by molecular weight, the identities of the hydrocarbons measured should be considered putative with the exception of isoprene [with mass *m* and charge number of ions *z* ratio, *m*/*z*, of 69] and monoterpenes (*m*/*z* of 137) that were validated using a gas chromatograph equipped with a mass selective (MS) detector (GC-MS). Concentrations of measured compounds were determined using a dynamic dilution technique that was applied before, during, and after the measurement campaign. We used a commercial gas standard in high-purity air (Apel-Riemer Environmental, Inc., Boulder, Colorado) containing 15 different compounds at mixing ratios of ~500 ppbv and diluted the standard using zero air via a catalytic converter (Restek, Inc., Bellefonte, Pennsylvania) and a series of mass flow controllers. After subtracting zero air from the measured counts per second, the average normalized counts per second (ncps), which were normalized by both *m*/*z* 21 and 37, were plotted against the gas mixing ratio at four different levels. The calibration factor (ncps/ppbv ± uncertainty) was then applied to our field measurements after subtracting intermittent zeros in order to obtain final concentration values. A fast mobility particle sizer (model 3091, TSI Inc., Shoreview, Minnesota) and a cloud condensation nuclei counter (CCN-100, Droplet Measurement Technologies Inc., Boulder, Colorado) recorded aerosol size and concentration and CCN number concentrations at 40 m above the forest canopy (Fig. 3; Table 1).

The investigation of canopy-level processes is linked to the thermodynamic state of the atmospheric boundary layer. Such links were determined using a tethered balloon that was capable of providing atmospheric profiles of temperature, relative humidity, ozone, and aerosol concentrations for air layers extending from the surface to 1,000 m above the ground (Fig. 1).

The datasets (Table 1) described above already exist on common repositories (https://psu.app.box.com/files/0/f/3492243782/NewGoAmazon). Once graduate students complete their preliminary analyses, the datasets and associated documentation will be placed on publicly accessed data banks, including the Department of Energy's Atmospheric Radiation Measurement (ARM) archives (www.archive.arm.gov/discovery/#v/home/s/) and Fluxnet (http://fluxnet.ornl.gov/). In the meantime, readers interested in seeking to use the resulting datasets may contact the corresponding author to get copies of required information with support of the coauthors.

OVERVIEW OF RESULTS. During 2014, the study site recorded a total rainfall of approximately 2,000 mm, with a clear seasonality in rainfall patterns. Monthly rainfall exceeded 250 mm from January through May but was as little as 50 mm during June–October. Mean monthly air temperature patterns exhibited a seasonal variation of less than 2°C, with the monthly average air temperature reaching 27°C (Fig. 4a). In addition to seasonal variations, there was a distinct diel pattern of air temperature and rainfall. The average range of the daily temperature cycle above the forest canopy often exceeded 6°C (Fig. 4b), larger than the annual

Table 1. Description of instruments employed during the field campaign and the environmental variables measured. The instruments were operated during the entire period (Jun 2014–Jan 2015) unless otherwise noted in the comments column.

Instrument	Variable	Measurement frequency (Hz)	Height or depth (m)	Comments
		Meteorological sensors		
Time domain reflectometers	Volumetric soil moisture content	1	−0.5 to −0.75	
Heat flux plates	Soil heat flux	1	−0.05	
Thermistor	Soil temperature	1	−0.5 to −0.75	
Infrared thermometer	Surface temperature	1	2.0, 34.9	
Wetness sensor	Leaf wetness	1	0.6, 1.9	
Sonic anemometer	Wind velocity, (u, v, w), and virtual temperature (T_v)	20	1.5, 7.0, 13.5, 18.4, 22.1, 24.5, 31.6, 34.9, 40.4, 48.2	
Pyranometer	Incoming solar irradiance	1	1.7, 39.0	
Pyrgeometer	Outgoing solar irradiance	1	1.7, 39.0	
Pyranometer	Incoming terrestrial irradiance	1	1.7, 39.0	
Pyrgeometer	Outgoing terrestrial irradiance	1	1.7, 39.0	
Thermistor	Air temperature	1	32.5	
Hygristor	Relative humidity	1	32.5	
		Gas and aerosol analyzers		
Infrared gas analyzer	Water vapor concentration	20	48.2, 1.5	The 48.2 value operated during Apr–May and Oct–Jan
Infrared gas analyzer	Carbon dioxide concentration	20	48.2, 1.5	The 48.2 value operated during Apr–May and Oct–Jan
Ultraviolet gas analyzer	Ozone mixing ratio	1	40.0	
	Carbon monoxide	1	40.0	
Gas analyzer	Sulfur dioxide	1	40.0	
Gas analyzer	Nitric oxide	1	40.0	
Gas analyzer	Nitrogen dioxide	1	40.0	
Fast mobility particle sizer	Aerosol size and concentration	1	40.0	25 Jun–2 Jul, 25 Jul–23 Aug, 26 Sep–4 Oct
CCN counter	CCN concentration	1	40.0	29 May–15 Jul, 28 Sep–15 Oct
Proton Reaction mass spectrometer	Isoprene and monoterpene concentration	1	40.0	Jun–Jan
		Tethered balloon		
Barometer	Pressure	1	1.5 to 800	16 Oct–12 Nov
Thermistor	Air temperature	1	1.5 to 800	16 Oct–12 Nov
Hygrsitor	Relative humidity		1.5 to 800	16 Oct–12 Nov
UV gas analyzer	Ozone	1	1.5 to 800	16 Oct–12 Nov
Aerosol probe	Aerosol size and concentration	1	1.5 to 800	16 Oct–12 Nov

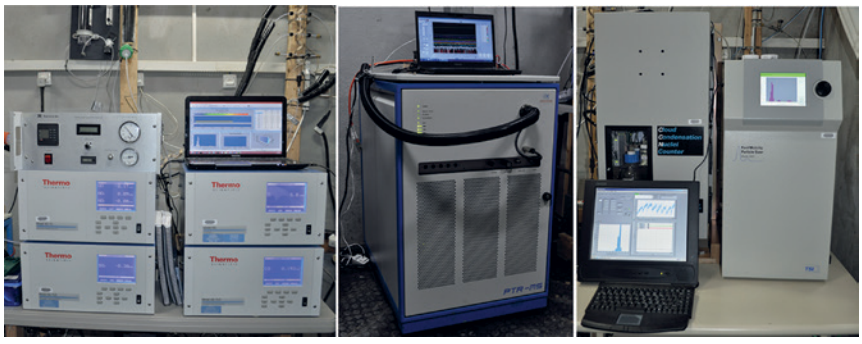

Fig. 3. (left) Analyzers of ozone, carbon monoxide, sulfur dioxide, and nitrogen oxides were used to investigate the chemistry within and above the rain forest canopy. (middle) A PTR-MS provided concentrations of hydrocarbons. A fast mobility particle sizer recorded the physical size and concentration of aerosols. (right) A CCN counter generated concentrations of CCN based on five supersaturation levels.

variation, which is important to understand emissions of rain forest–emitted hydrocarbons, which depend on foliage temperature (e.g., Fuentes et al. 2000). The daily cycle of mean rainfall showed two distinct maxima that were caused by the preferential development of rain events in the early morning hours [around 0400 local time (LT)], which was most likely associated with organized convective systems that propagated into the interior of the Amazon from the east with a large stratiform rain component, and a second, stronger maximum in the afternoon (1200–1600 LT) that was linked to locally generated convection. The afternoon rain maximum was more pronounced in the dry season (June–September) than in the wet season, during which rainfall was more evenly distributed throughout the course of the day (Fig. 4). Mesoscale convective storms and squall lines produced rain rates of more than 20 mm h^{-1}.

The observed seasonality in rainfall influenced the available energy (i.e., R_{Net}) above the forest. Because of its tropical location, the site received large amounts of solar radiation input that at times approached and exceeded the solar constant (Gu et al. 2001). During the most intense period of the rainy season, maximum net radiation of about 650 W m^{-2} was recorded as a result of increased cloud cover, compared to approximately 750 W m^{-2} during October (Fig. 5). At the same time, the impact of locally generated convection could be observed during the dry season as midday convective systems contributed to reductions of incoming solar irradiance. In October 2014, these events occurred frequently and gave rise to not only copious cloud cover and rain but also strong wind gusts above the canopy. Figure 5 also shows that approximately half of the available energy was partitioned into evapotranspiration (i.e., *LE*). Maximum *LE* reached approximately 400 W m^{-2}, whereas *H* was often approximately 100 W m^{-2} during the midday. These energy fluxes operated in a highly turbulent environment at the canopy top during the daytime. The soil heat flux had a midday average of less than 10 W m^{-2} (Fig. 5) and was negligible compared to the net radiation measured above the forest canopy. The sum of *H* and *LE* is substantially less than the net radiation, and this fact reflects that other components (energy in the biomass or canopy air space) of the surface energy balance need to be considered for this type of ecosystem.

Air turbulence controls the vertical transport and the distribution of rain forest–emitted hydrocarbons in the atmospheric boundary layer. As shown by u_* values (Fig. 6), atmospheric turbulence exhibited

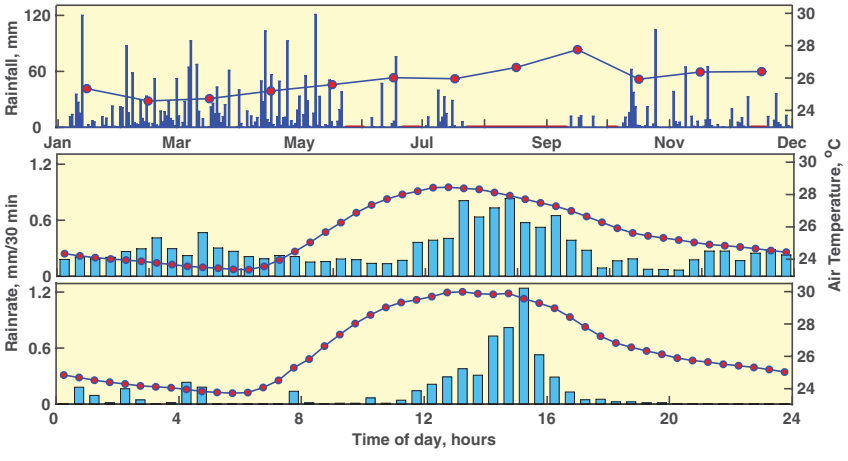

Fig. 4. (top) Seasonal patterns in rainfall (purple bars, total daily amounts) and monthly mean air temperature measured at 40 m above the ground (red markers indicate missing rainfall data). Diel variations of rainfall rate (light blue bars) and air temperature at the study site during (middle) the wet season and (bottom) the dry season (Jun–Sep).

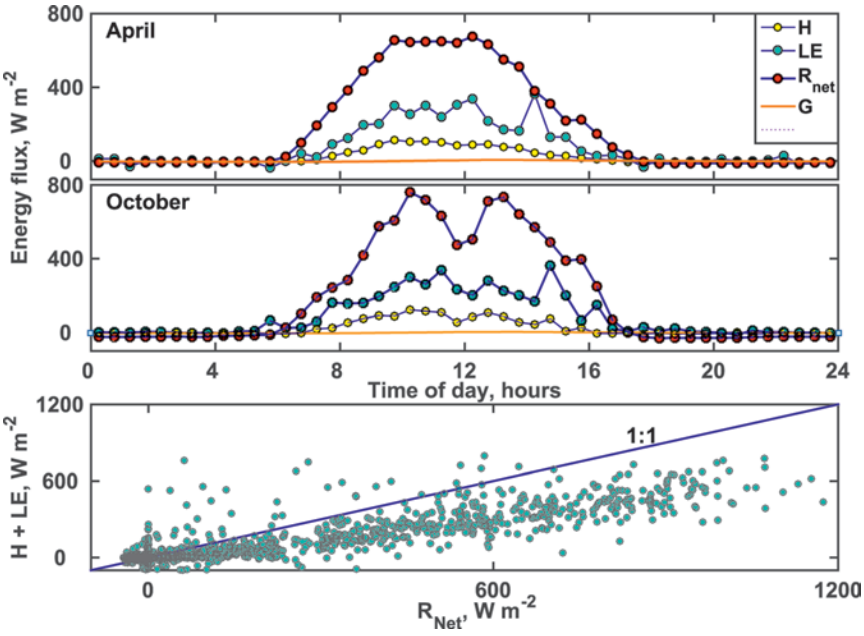

Fig. 5. Diel cycles of the surface energy balance components: net radiation R_{Net}, sensible heat flux *H*, latent heat flux *LE*, and soil heat flux *G* during (top) Apr and (middle) Oct, as well as (bottom) the relationship between R_{Net} and the sum of the turbulent heat fluxes (*H* + *LE*).

pronounced diel cycles with maximum u_* values of about 0.5 m s^{-1} observed by the middle of the day in response to strong wind shear above the forest. During the nighttime, quiescent periods dominated and u_* remained around 0.15 m s^{-1}. Such air turbulence characteristics allowed trace gases to be relatively well mixed during the daytime and poorly distributed during the nighttime in the atmospheric boundary layer.

Knowledge of air turbulence within and above the forest can help explain the distribution of gases and associated surface deposition rates. The vertical variation of turbulence statistics, such as σ_w, exhibited a strong variability within the forest canopy throughout the course of the day (Fig. 7). For example, during the middle of the day, above the forest canopy, the mean σ_w maximum reached 0.6 m s^{-1}, whereas in the lower regions of the canopy the σ_w remained below 0.05 m s^{-1}. The σ_w decreased rapidly from the top to the bottom of the canopy in response to the effective momentum dissipation by the foliage in the upper regions of the canopy. Above the canopy, the σ_w remained nearly invariant. Within the lower regions of the forest canopy, the σ_w values ranged from 0.03 to 0.3 m s^{-1} in response to the attenuation of the vertical velocity fluctuations because of the drag force exerted by the forest. The smallest σ_w values (<0.3 m s^{-1}) prevailed in the air layer from the forest floor to z/hc = 0.65. The reduced eddy motion within the canopy resulted because of the momentum sink in the upper canopy and eddies became weak and inactive within the deeper forest trunk space. Vertical variations of σ_w serve as indicators of the turbulence potential of realizing gas transport out of and into the forest canopy. Also, turbulent statistics within the forest (Fig. 7) provide critical information for the interpretation of the coupling or decoupling of the canopy and the overlying atmosphere and among different layers within the forest. Nighttime low levels of turbulence allowed the accumulation of emitted gases within the canopy and

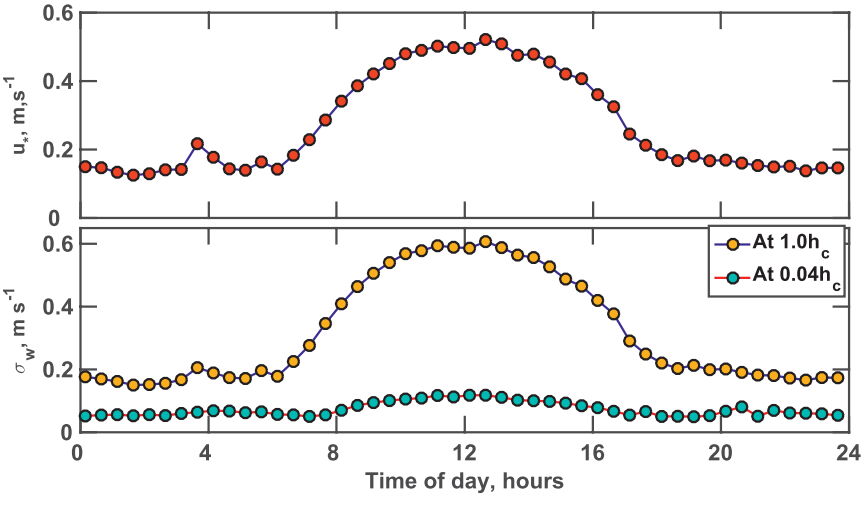

Fig. 6. (top) Diel cycles of average friction velocity at the canopy top (30 m) during Apr 2014–Jan 2015. (bottom) Diel cycles of average standard deviation of the vertical velocity at the canopy top (cyan) and at 1.5 m above the ground surface (orange).

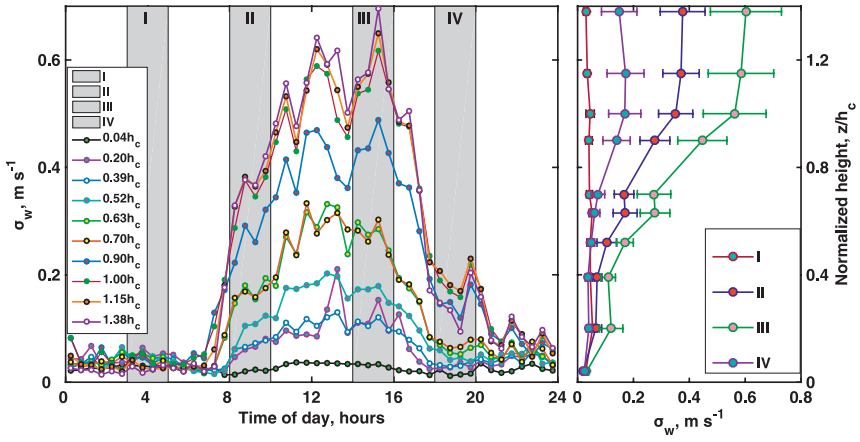

Fig. 7. (left) Temporal variations of the standard deviation of the vertical velocity determined at different levels above the surface during 1 Dec 2015. (right) Vertical variations of the vertical velocity standard deviation for periods (I–IV) exhibiting different degrees of atmosphere–forest coupling.

limited the transport of gases from above to within the canopy. As a consequence, air masses above the canopy exhibited different chemical composition attributes compared to the less well-mixed air within the canopy (see below). During the transition period from nighttime to daytime, the turbulence progressively increased, reaching the lower half of the canopy about 1.5 h after sunrise. This enhanced the mixing of scalars and exchanges of in-canopy air with the overlying atmosphere. The two air layers remained strongly coupled during most of the daytime until the levels of turbulence were again reduced after sunset (Fig. 7).

Ozone is one of the principal oxidants of hydrocarbons during the rainy season in the remote regions of the tropical rain forest. In the atmospheric boundary layer, ozone is produced from photochemical reactions entailing nitrogen oxides. Tropical soils emit some nitric oxide (NO), which can rapidly react with ozone to form nitrogen dioxide (NO_2); during the daytime the resulting NO_2 undergoes photolysis to produce the atomic oxygen needed to form ozone. Moreover, the downdrafts associated with convective storms transport ozone from the middle troposphere to the surface (e.g., Betts et al. 2002). In response to these two primary ozone sources, large differences (e.g., 10 ppbv) exist between the ozone mixing ratios measured above the forest during disturbed days with rain events and undisturbed days without. During disturbed periods, the atmospheric boundary layer is strongly linked to the free troposphere. In the wet season, the ozone mixing ratios remained relatively low as a result of reduced photochemical processes associated with increased cloudiness (Fig. 5) and precipitation (Fig. 4), with average maximum ozone levels only reaching 15 ppbv around the middle of the day (Fig. 8). In contrast, the average maximum ozone mixing ratios during the dry season commonly reached 20 ppbv and the time at which the maximum ozone levels occurred shifted from 1500 to 1600 LT, which is indicative of both greater photochemistry and the long-range transport of polluted air masses. Ozone levels were also higher during the dry season because of greater photochemical production involving the increased presence of regional biomass burning that often created plumes laden with nitrogen oxides and carbon monoxide (Andreae et al. 2004).

The Amazon rain forest represents not only the largest source of hydrocarbons on Earth but also emits a great variety of chemical species. Based on the PTR-MS measurements, dominant hydrocarbons observed

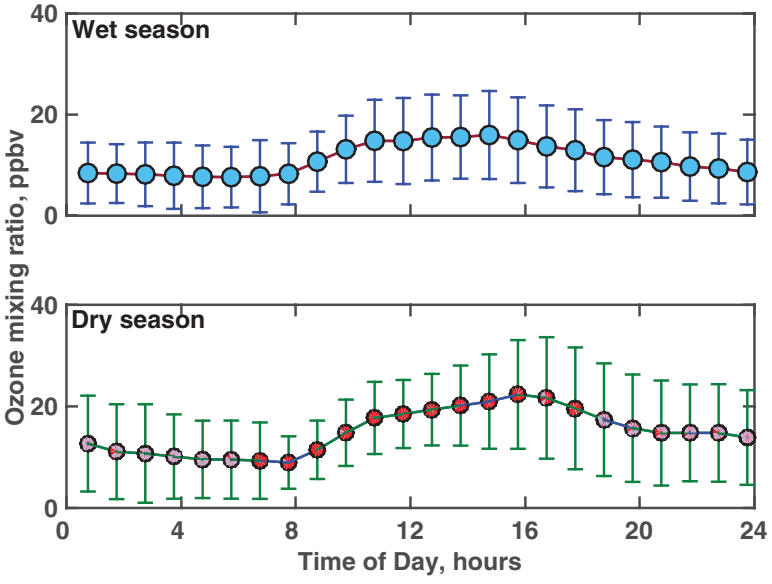

Fig. 8. Average hourly ozone mixing ratio and standard deviation measured above the rain forest during the wet and dry seasons.

above the rain forest included methanol (52%), isoprene (13%), acetone (12%), acetaldehyde (12%), and monoterpenes (3%) [Fig. 9; see also Gerken et al. (2016); Jardine et al. (2015)]. For comparison, during the middle of the growing season the temperate forests in North American emit mostly isoprene (51%) and terpenes (31%) (Fuentes et al. 2000). Most of the identified chemical species in Fig. 9 are emitted from vegetation. The exceptions are methyl vinyl ketone (MVK) and methacrolein (MACR), which are largely generated from the oxidation of isoprene, although some plant species are known to emit these gases (Jardine et al. 2013). The PTR-MS measurements do not resolve specific monoterpene species. However, based on previous studies at the same study site, the rain forest produces at least 12 different monoterpene species, including β-ocimene and terpinolene, which are highly reactive with respect to ozone (Jardine et al. 2015).

In the rain forest, biogenic volatile organic compounds (BVOCs) play important roles in driving the air chemistry in the atmospheric boundary layer. As noted earlier (Fig. 9), the ambient mixing ratios of rain forest–produced hydrocarbons exhibited strong temporal patterns in response to the environmental and plant physiological conditions controlling emissions. For example, isoprene had the highest mixing ratios above the forest canopy during 1200–1500 LT, with maximum averaged mixing ratios of 6 ppbv (Fig. 10) during the wet season. Isoprene emissions depend on foliage temperature and incident photosynthetic active irradiance and the diffusion of isoprene molecules from sites of biosynthesis (i.e., chloroplast) to stomatal cavities. Therefore, plant physiological activity such as stomatal opening or closing and carbon assimilation rates can control the emission of isoprene to the atmosphere as molecules are produced within chloroplasts (Fuentes et al. 2000). During the early dry season, lower BVOC mixing ratios prevailed in response to reduced emissions from young leaves (Barkley et al. 2009; Kuhn et al. 2004). During the nighttime, isoprene levels within the canopy volume did not vanish but attained a minimum of about 1 ppbv that can be ascribed to some vertical transport from aloft to the surface (e.g., Fuentes et al. 1996). Monoterpene mixing ratios also exhibited strong temporal patterns throughout the day in response to sources from vegetation and sinks due to surface deposition and chemical reactions. During the wet season, maximum monoterpene mixing ratios of approximately 1.0 ppbv were observed during 1200–1500 LT (Fig. 10) as a result of the strong emissions that are largely controlled by foliage temperature (Fuentes et al. 2000). Emissions of some monoterpenes (e.g., β-ocimene) can also be influenced by photosynthetic-active irradiance impinging on foliage (Jardine et al. 2015).

The vertical distribution of gases within and above the rain forest depends on the source strength of the emissions, the distribution of the sources and sinks, and the characteristics of the air turbulence. For example, ozone mixing ratios monotonically decreased with canopy depth (Fig. 11) as a result of chemical reactions with hydrocarbons and the deposition to foliage elements. Within the canopy, during the rainy season ozone sinks dominated and there was limited ozone formation as a result of the near absence of nitrogen oxides (data not shown). From the forest floor to about 20 m above the surface (Fig. 11), ozone levels remained considerably lower than in the upper canopy. In part, this distribution of ozone resulted because of turbulence characteristics in the forest canopy. As demonstrated by the vertical profiles of σ_w (Figs. 7 and 11), the lower region of the

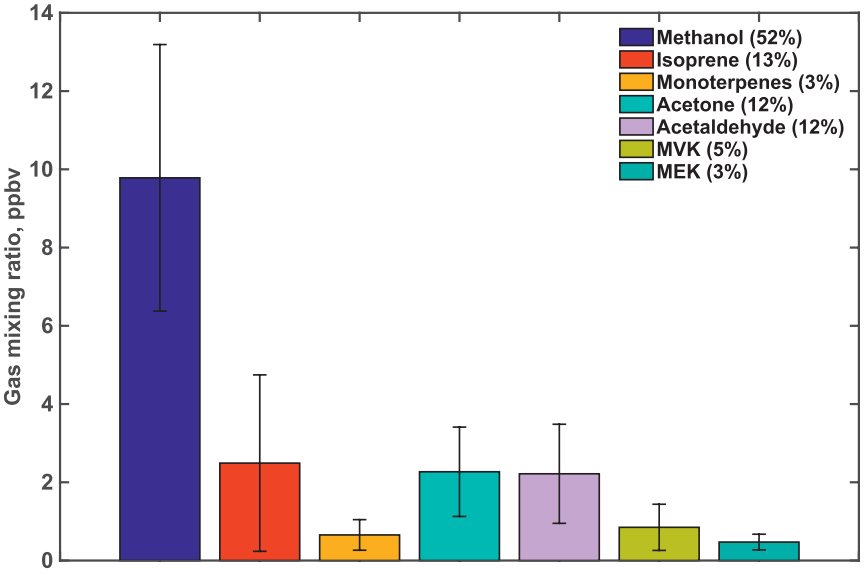

Fig. 9. Averaged gas mixing ratios and associated standard deviation of the principal chemical species measured above the rain forest during the 2014 wet and dry seasons. MVK refers to the sum of methyl vinyl ketone and methacrolein.

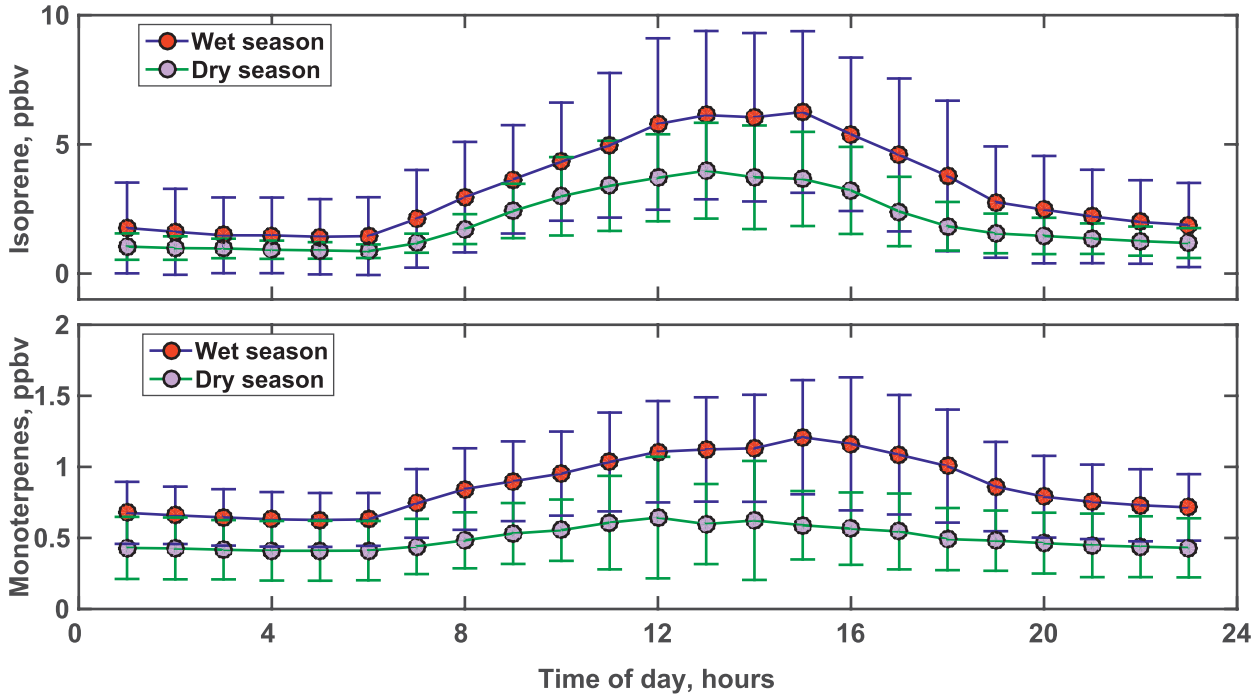

Fig. 10. Diel cycles of average (top) isoprene and (bottom) monoterpene mixing ratios measured above the rain forest during two periods from 19 Dec 2014 to 16 Jan 2015 (wet season) and 16 Jun to 1 Jul 2015 (early dry season). The whiskers around the symbols indicate one standard deviation.

canopy remained in a poorly mixed state and at times was largely decoupled from the air layers above the canopy and, as a consequence, the transport of trace gases was inhibited.

In contrast to ozone, the distribution of sources within the canopy largely controlled the vertical variation of rain forest–emitted isoprene and monoterpenes. For instance, isoprene and monoterpene exhibited maximum mixing ratios within the forest crown (where the leaf area density was near its maximum). This region of the canopy had the largest amount of active biomass [Jardine et al. (2015); Tóta et al. (2012); the leaf area density included in Fig. 11 came from Tóta et al. (2012)] contributing to hydrocarbon emissions. Also, during the daytime, the largest interception of photosynthetic active irradiance and maximum foliage temperature occurred in the upper region of the canopy, driving hydrocarbon emissions. Atmospheric turbulence, as expressed in the σ_w profiles (Fig. 11), was sufficiently strong to transport hydrocarbons away from sources that were positioned in the upper third of the canopy. The distribution of trace gases, coupled with air turbulence characteristics, indicated that the rain forest canopy provided an environment suitable for driving the chemical reactions that contributed to the formation of particles (see below).

Above the rain forest, the levels of trace gases and aerosols varied with altitude in response to atmospheric stability–instability and sources and sinks. Using data obtained with the tethered balloon during statically stable conditions (i.e., periods during which virtual potential temperature increased with altitude, typical for nighttime conditions), Fig. 12 provides an example of rapidly increasing ozone mixing ratios with altitude [by about 0.02 ppbv (5 m)$^{-1}$ in the air layers adjacent to the forest in response to surface removal and reactions with hydrocarbons]. During stable conditions, the air layer extending from the surface to about 250 m (the depth of the stable boundary layer) above the ground experienced the most rapid ozone loss in response to sink processes. The distribution of trace gases and aerosols (data not shown) was constantly evolving within the stable boundary layer as a result of surface deposition, air chemistry, and turbulence.

A case study illustrates the interplay of hydrocarbon emissions, air chemistry, and atmospheric turbulence that could lead to the formation of cloud condensation nuclei. Mesoscale convective systems or squall lines downwardly transported and regionally enhanced the atmospheric boundary layer with ozone. For example, around 0100 LT ozone levels increased from 5 to 15 ppbv in response to the passage of a storm, which produced a rain rate of 10 mm (30 min)$^{-1}$, with a smaller increase in ozone when another storm passed over the site at

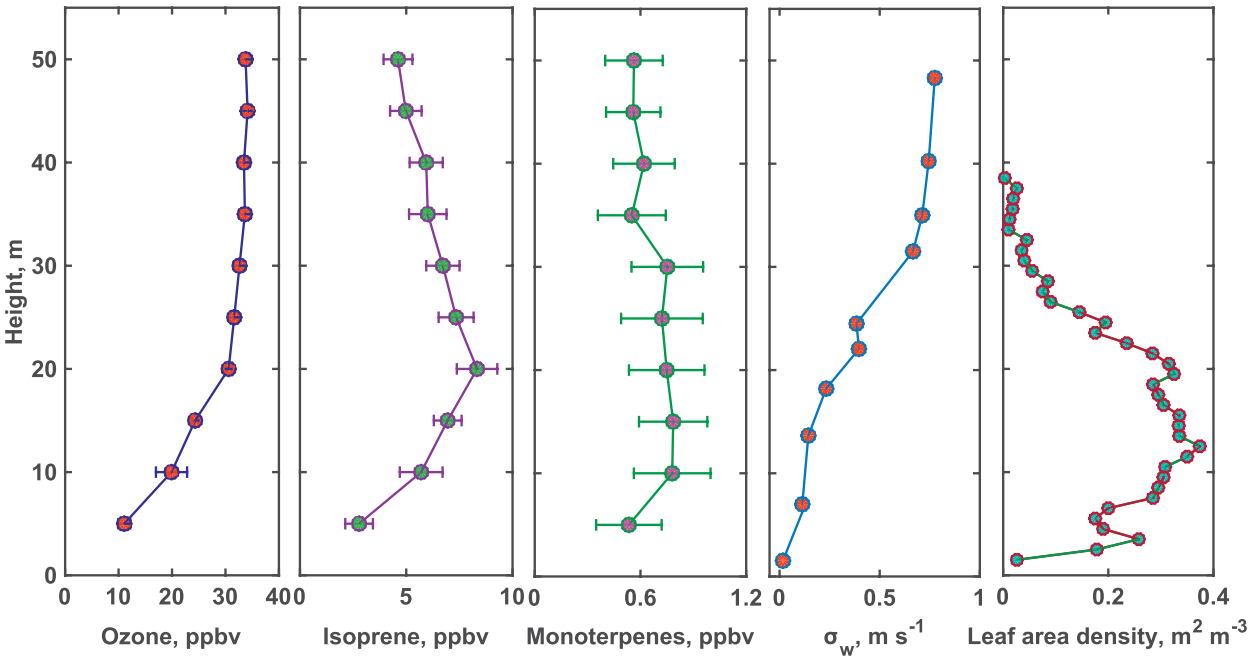

Fig. 11. Vertical variation of ozone, isoprene, monoterpenes, and the standard deviation of the vertical velocity measured during 30 Oct 2014 for a period of 50 min starting at 0859 LT. The circles provide 5-min averages, and the bars represent the standard deviation around the mean values. The forest leaf area density (m^2 m^{-3}) at the study site is also included.

0400 LT (Fig. 13). Incoming solar irradiance started to appreciably increase around 1000 LT as a result of decreases in the cloud cover. At the same time, isoprene and monoterpene emissions gave rise to maximum mixing ratios of 11.0 and 1.2 ppbv, respectively, around 1300 LT. Meanwhile, the CCN concentration gradually increased in the morning hours and attained the maximum concentration of 275 particles cm^{-3} (Fig. 13).

In the rain forest, storms routinely and substantially modify the photochemical processes responsible for the oxidation of hydrocarbons and the formation of aerosols. For example, at 1330 LT (Fig. 13) the ozone levels increased from 8 to 19 ppbv as a mesoscale convective system passed by the study site. Downward-moving air parcels transported ozone-rich air to the surface. Air parcels emanated from 2 to 3 km above the ground as demonstrated by the rapid movement of air and the magnitude of the equivalent potential temperature (θ_e) decline [the θ_e is used as a tracer because it is conserved in the condensation and evaporation of water; Betts et al. (2002)]. Isoprene and monoterpenes abruptly declined as descending air parcels transported nearly hydrocarbon-depleted air around 1330 LT. Following the storm, the isoprene levels reached about 1.5 ppbv in

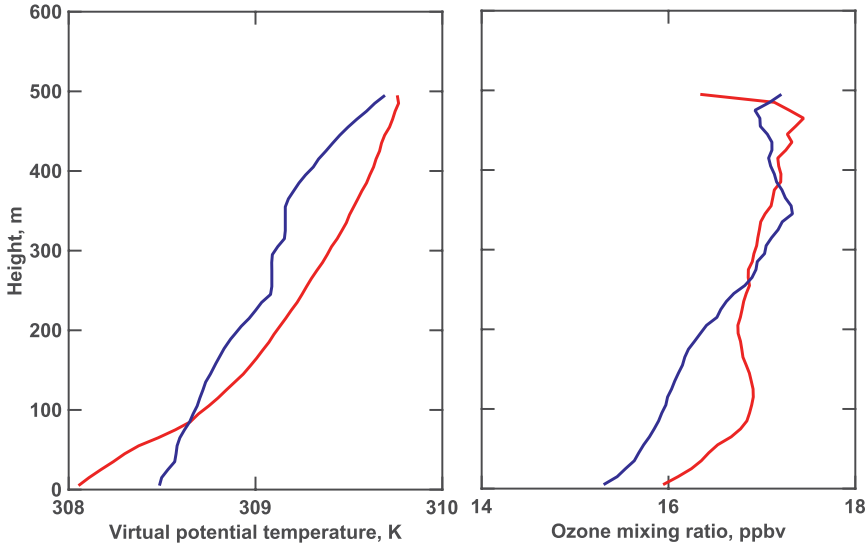

Fig. 12. Vertical variation of virtual potential temperature and ozone from 0050 (blue line) to 0150 LT (red line) 9 Nov 2014. Measurements were made with sensors mounted on a sonde carried by a tethered balloon.

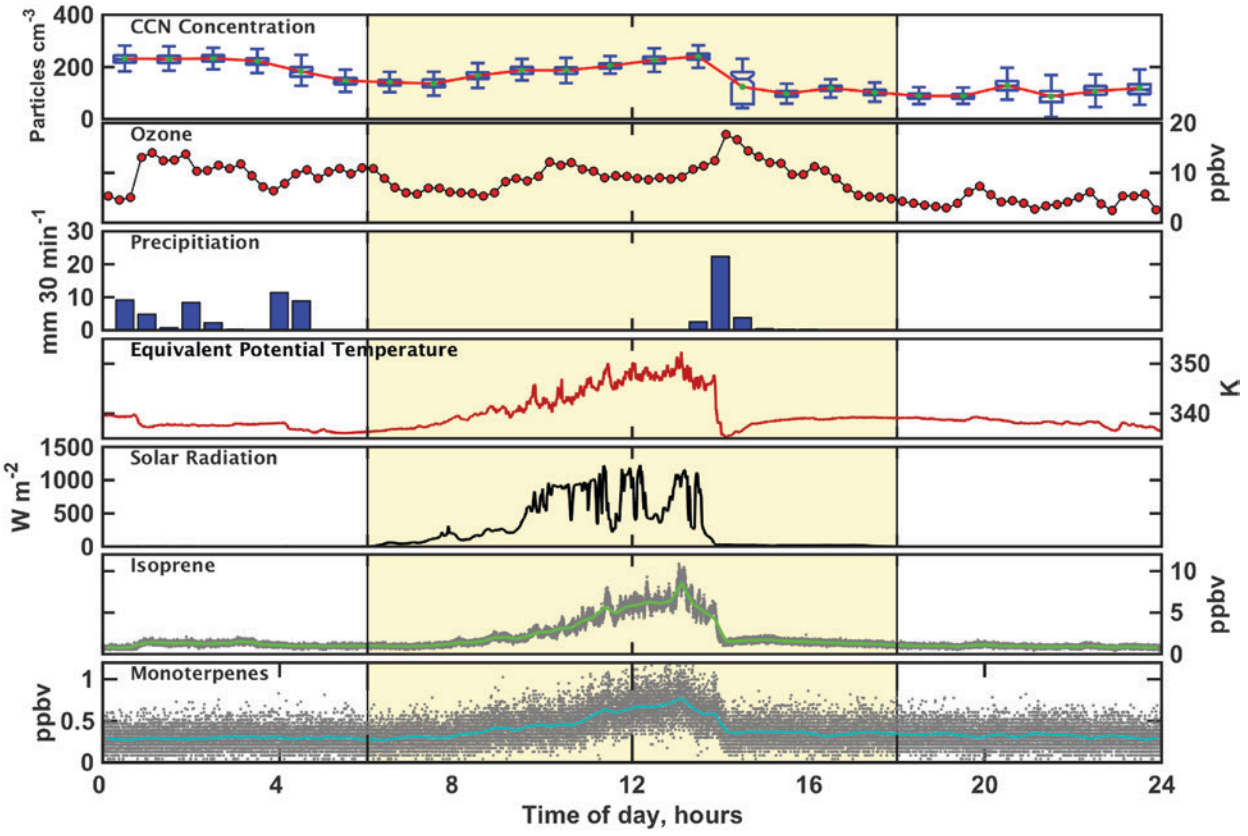

Fig. 13. Diel cycles of monoterpenes, isoprene, solar irradiance, equivalent potential temperature (θ_e), rain rate, ozone mixing ratio, and concentration of CCN on 18 Jun 2014 (please see text for explanation of data).

response to low emissions caused by the limited solar irradiance (of about 100 W m^{-2}), whereas monoterpene mixing ratios attained 0.3 ppbv (Fig. 13). Also, the concentration of CCN rapidly decreased from a maximum concentration of 275 particles cm^{-3} to a minimum concentration of 50 particles cm^{-3} in response to both rain out and the transport of cleaner air from aloft. After the storm, hydrocarbon emissions resumed, albeit at much reduced rates compared to the ones during 1000–1200 LT. Subsequent reactions involving the enhanced ozone (varying from 18 to 5 ppbv during 1330–1800 LT) and hydrocarbons, but principally monoterpenes (whose mixing ratios stayed around 0.3 ppbv), generated substantial amounts of hydroxyl radicals (Gerken et al. 2016), which additionally contributed to the oxidation of the hydrocarbons. With these datasets (Fig. 13), we intend to investigate the oxidation rates of plant-emitted hydrocarbons and the formation of aerosols using analyses and photochemical models. Of great interest is determining the yields of secondary organic aerosols from hydrocarbon oxidation and the subsequent activation of aerosols into CCNs immediately after the occurrences of mesoscale convective storms.

SUMMARY. The Amazonian rain forest emits large amounts of diverse hydrocarbons. Dominant gas species include methanol, isoprene, acetone, monoterpenes, acetaldehyde, and the isoprene reaction products methyl vinyl ketone and methacrolein. Emissions are strong enough to give rise to maximum isoprene and monoterpene mixing ratios of greater than 15 and 2 ppbv, respectively. As revealed by atmospheric turbulence characteristics, there are prolonged times when the lower regions of the canopy remain quiescent. Under such conditions, ozone remains mostly depleted in the lower levels of the canopy because of reactions with hydrocarbons and surface deposition. Conversely, during statically unstable conditions, ozone and hydrocarbons stay relatively well mixed in the canopy as a result of high turbulence levels. Given the limited actinic irradiance required to drive photochemical processes, ozone and hydrocarbons principally initiate the reactions within and above the rain forest during the wet season. During the rainy season, the regional atmospheric boundary layer is routinely enriched with ozone because of the downward transport generated by the downdrafts of squall lines and mesoscale convective storms. Reactions of ozone

with hydrocarbons generate substantial amounts of hydroxyl radicals (data not shown), which additionally contribute to the oxidation of hydrocarbons. In the wet season, reactions of ozone and hydroxyl radicals with rain forest–emitted hydrocarbons play crucial roles in the oxidation of plant-emitted hydrocarbons (Gerken et al. 2016). The field project described herein generated rare datasets (Table 1) that may be used to investigate the links between meteorology, atmospheric turbulence, and air chemistry. Ongoing data analyses and numerical modeling studies are focusing on whether the rain forest produces the necessary chemical species and in sufficient amounts to undergo oxidation and generate aerosols that subsequently activate into cloud condensation nuclei.

ACKNOWLEDGMENTS. The U.S. Department of Energy supported the field studies as part of the GoAmazon project (Grant SC0011075). Fundação de Amparo à Pesquisa do Estado de São Paulo (FAPESP) and Fundação de Amparo à Pesquisa do Estado do Amazonas (FAPEAM) funded the Brazilian component of the field studies. The authors acknowledge the support from the Central Office of the Large-Scale Biosphere-Atmosphere Experiment in Amazonia (LBA), the Instituto Nacional de Pesquisas da Amazonia (INPA), and the Universidade do Estado do Amazonia (UEA). The work was conducted under 001030/2012-4 of the Brazilian National Council for Scientific and Technological Development (CNPq). The Office of the LBA provided logistic support and made the flux tower and housing unit available to complete the field studies. The authors acknowledge support from the Duke WISeNet Program sponsored by the National Science Foundation (Grant DGE-1068871). The field project would have not been possible without the assistance of several Brazilian undergraduate and graduate students, including from INPE Diego Jatoba dos Santos Jelena Maksic and Theomar Trindade de Araújo Tiburtino Neves; from UFSM Daniel Michelon dos Santos, Gustavo Pujol Veeck, and Pablo E. S. Oliveira; from UFPR Bianca Luhm Crivellaro, Einara Zahn, Fernando Armani, Lucas Hoeltgebaum, and Vanessa Monteiro; from UEA Amne Sampaio Fredó, Ariana Almeida Gomes, Bianca Cristina Pinto Hassan, Claudomiro Batista Sales, Evandro Alves de Carvalho Jr., Francisco Otávio Miranda Farias, Igor Bruno Carramanho de Azevedo, Leandra Gomes de Aguiar, Luan Rogério Rodrigues Carvalho, Milena Vieira, Nikolai da Silva Espinoza, Priscila Pereira de Miranda, Raoni Aquino Silva de Santana, Roseilson Souza do Vale, Tanya Debora Bezerra de Castro, and Tatiana Rolin da Fonseca; from UFOPA Adriane Cristina dos Santos Oliveira, Carolina Stefani Rodrigues da Rocha, Gabriel Vidal Mota, Giorgio Arlan S. Picanco, Juliana Amaral Vinholte, and Rardiles Branches Ferreira; from UBRA Rodrigo Gomes da Silva; and from FDB Antônio Huxley Melo do Nascimento. The authors thank two anonymous reviewers for recommending revisions that considerably improved manuscript. Two anonymous reviewers provided substantial comments that helped to improve the original manuscript. The authors thank the editor, Peter Blanken, for his timely processing of the manuscript.

REFERENCES

Andreae, M. O., 2009: A new look at aging aerosols. *Science*, **326**, 1493–1494, doi:10.1126/science.1183158.

——, and Coauthors, 2002: Biogeochemical cycling of carbon, water, energy, trace gases, and aerosols in Amazonia: The LBA-EUSTACH experiments. *J. Geophys. Res.*, **107**, 8066, doi:10.1029/2001JD000524.

——, D. Rosenfeld, P. Artaxo, A. A. Costa, G. P. Frank, K. M. Longo, and M. F. Silva-Dias, 2004: Smoking rain clouds over the Amazon. *Science*, **303**, 1337–1342, doi:10.1126/science.1092779.

Barkley, M. P., P. I. Palmer, I. De Smedt, T. Karl, A. Guenther, and M. Van Roozendael, 2009: Regulated large-scale annual shutdown of Amazonian isoprene emissions? *Geophys. Res. Lett.*, **36**, L04803, doi:10.1029/2008GL036843.

Betts, A. K., L. V. Gatti, A. M. Cordova, M. A. F. Silva Dias, and J. D. Fuentes, 2002: Transport of ozone to the surface by convective downdrafts at night. *J. Geophys. Res.*, **107**, 8046, doi:10.1029/2000JD000158.

Dupont, S., and Y. Brunet, 2009: Coherent structures in canopy edge flow: A large-eddy simulation study. *J. Fluid Mech.*, **630**, 93–128, doi:10.1017/S0022112009006739.

Finnigan, J. J., 2000: Turbulence in plant canopies. *Ann. Rev. Fluid Mech.*, **32**, 519–571, doi:10.1146/annurev.fluid.32.1.519.

Fuentes, J. D., D. Wang, G. den Hartog, H. H. Neumann, and T. F. Dann, 1996: Ambient biogenic hydrocarbon concentrations and isoprene emissions from deciduous forests. *J. Atmos. Chem.*, **25**, 67–95, doi:10.1007/BF00053286.

——, and Coauthors, 2000: Biogenic hydrocarbons in the atmospheric boundary layer: A review. *Bull. Amer. Meteor. Soc.*, **81**, 1537–1575, doi:10.1175/1520-0477(2000)081<1537:BHITAB>2.3.CO;2.

——, D. Wang, D. R. Bowling, M. Potosnak, R. K. Monson, W. S. Goliff, and W. R. Stockwell, 2007: Biogenic hydrocarbon chemistry within and above a mixed deciduous forest. *J. Atmos. Chem.*, **56**, 165–185, doi:10.1007/s10874-006-9048-4.

Gerken, T., and Coauthors, 2016: Downward transport of ozone rich air and implications for atmospheric chemistry in the Amazon rainforest. *Atmos. Environ.*, **124**, 64–76, doi:10.1016/j.atmosenv.2015.11.014.

Gu, L., J. D. Fuentes, M. Garstang, J. Tota da Silva, R. Heitz, J. Sigler, and H. H. Shugart, 2001: Cloud modulation of surface solar irradiance at a pasture site in southern Brazil. *Agric. For. Meteor.*, **106**, 117–129, doi:10.1016/S0168-1923(00)00209-4.

Guenther, A. B., and Coauthors, 1995: A global model of natural volatile organic compound emissions. *J. Geophys. Res.*, **100**, 8873–8892, doi:10.1029/94JD02950.

Jardine, A. B., and Coauthors, 2015: Highly reactive light-dependent monoterpenes in the Amazon. *Geophys. Res. Lett.*, **42**, 1576–1583, doi:10.1002/2014GL062573.

Jardine, K., and Coauthors, 2011: Within-canopy sesquiterpene ozonolysis in Amazonia. *J. Geophys. Res.*, **116**, D19301, doi:10.1029/2011JD016243.

——, and Coauthors, 2013: Emissions of putative isoprene oxidation products from mango under abiotic stress. *J. Exp. Bot.*, **64**, 3669–3679, doi:10.1093/jxb/ert202.

Kaimal, J. C., and J. E. Gaynor, 1991: Another look at sonic thermometry. *Bound.-Layer Meteor.*, **56**, 401–410, doi:10.1007/BF00119215.

——, and J. J. Finnigan, 1994: *Atmospheric Boundary Layer Flows: Their Structure and Measurement*. Oxford University Press, 289 pp.

Katul, G., A. Porporato, D. Cava, and M. Siqueira, 2006: An analysis of intermittency, scaling, and surface renewal in atmospheric surface layer turbulence. *Physica D*, **215**, 117–126, doi:10.1016/j.physd.2006.02.004.

Kesselmeier, J., and Coauthors, 2002: Concentrations and species composition of atmospheric volatile organic compounds (VOCs) as observed during the wet and dry season in Rondônia (Amazonia). *J. Geophys. Res.*, **107**, 8053, doi:10.1029/2000JD000267.

Kruijt, B., Y. Malhi, J. Lloyd, A. D. Norbre, A. C. Miranda, M. G. P. Pereira, A. Culf, and J. Grace, 2000: Turbulence statistics above and within two Amazon rain forest canopies. *Bound.-Layer Meteor.*, **94**, 297–331, doi:10.1023/A:1002401829007.

——, and Coauthors, 2002: Isoprene and monoterpene emissions of Amazonian tree species during the wet season: Direct and indirect investigations on controlling environmental functions. *J. Geophys. Res.*, **107**, 8071, doi:10.1029/2001jd000978.

Kuhn, U., and Coauthors, 2004: Seasonal differences in isoprene and light-dependent monoterpene emission by Amazonian tree species. *Global Change Biol.*, **10**, 663–682, doi:10.1111/j.1529-8817.2003.00771.x.

Machado, L. A. T., and Coauthors, 2014: The Chuva Project: How does convection vary across Brazil? *Bull. Amer. Meteor. Soc.*, **95**, 1365–1380, doi:10.1175/BAMS-D-13-00084.1.

Marques Filho, A. O., R. G. Dallarosa, and V. P. Pacheco, 2005: Radiação solar e distribuição vertical de área foliar em floresta: Reserva Biológica do Cuieiras—ZF2, Manaus. *Acta Amazonica*, **35**, 427–436, doi:10.1590/S0044-59672005000400007.

Martin, S. T., and Coauthors, 2010: Sources and properties of Amazonian aerosol particles. *Rev. Geophys.*, **48**, RG2002, doi:10.1029/2008RG000280.

——, and Coauthors, 2016: Introduction: Observations and Modeling of the Green Ocean Amazon (GoAmazon2014/5). *Atmos. Chem. Phys.*, **16**, 4785–4797, doi:10.5194/acp-16-4785-2016.

Nobre, C. A., P. J. Sellers, and J. Shukla, 1991: Amazonian deforestation and regional climate change. *J. Climate*, **4**, 957–988, doi:10.1175/1520-0442(1991)004<0957:ADARCC>2.0.CO;2.

Pöschl, U., and Coauthors, 2010: Rainforest aerosols as biogenic nuclei of clouds and precipitation in the Amazon. *Science*, **329**, 1513–1516, doi:10.1126/science.1191056.

Roberts, G. C., M. O. Andreae, J. Zhou, and P. Artaxo, 2001: Cloud condensation nuclei in the Amazon basin: "Marine" conditions over a continent? *Geophys. Res. Lett.*, **28**, 2807–2810, doi:10.1029/2000GL012585.

Strong, C., J. D. Fuentes, and D. Baldocchi, 2004: Reactive hydrocarbon flux footprints during canopy senescence. *Agric. For. Meteor.*, **127**, 159–173, doi:10.1016/j.agrformet.2004.07.011.

Tóta, J., D. R. Fitzjarrald, and M. A. F. da Silva Dias, 2012: Amazon rainforest exchange of carbon and subcanopy air flow: Manaus LBA site—A complex terrain condition. *Sci. World J.*, **2012**, 1–19, doi:10.1100/2012/165067.

Werth, D., and R. Avissar, 2002: The local and global effects of Amazon deforestation. *J. Geophys. Res.*, **107**, 8087, doi:10.1029/2001JD000717.

Williams, E., and Coauthors, 2002: Contrasting convective regimes over the Amazon: Implications for cloud electrification. *J. Geophys. Res.*, **107**, 8280, doi:10.1029/2001JD000380.

Zimmerman, P. R., J. P. Greenberg, and C. E. Westberg, 1988: Measurements of atmospheric hydrocarbons and biogenic emission fluxes in the Amazon boundary layer. *J. Geophys. Res.*, **93**, 1407–1416, doi:10.1029/JD093iD02p01407.